

## STABILITY OF A NANOFILTRATION MEMBRANE AFTER CONTACT WITH A LOW-LEVEL LIQUID RADIOACTIVE WASTE

Elizabeth Eugenio de Mello Oliveira and Celina Cândida Ribeiro Barbosa

Instituto de Engenharia Nuclear, Rua Hélio de Almeida, 75, Ilha do Fundão, 21941-614 Rio de Janeiro – RJ, Brasil

Júlio Carlos Afonso\*

Departamento de Química Analítica, Instituto de Química, Universidade Federal do Rio de Janeiro, Av. Athos da Silveira Ramos, 149, Ilha do Fundão, 21941-909 Rio de Janeiro – RJ Brasil

Recebido em 2/4/13; aceito em 4/7/13; publicado na web em 21/8/13

This study investigated the treatment of a liquid radioactive waste containing uranium ( $^{235}\text{U}$  +  $^{238}\text{U}$ ) using nanofiltration membranes. The membranes were immersed in the waste for 24–5000 h, and their transport properties were evaluated before and after the immersion. Surface of the membranes changed after immersion in the waste. The SW5000 h specimen lost its coating layer of polyvinyl alcohol, and its rejection of sulfate ions and uranium decreased by about 35% and 30%, respectively. After immersion in the waste, the polyamide selective layer of the membranes became less thermally stable than that before immersion.

Keywords: uranium; nanofiltration; waste treatment.

### INTRODUCTION

In a membrane separation process (MSP), application of a chemical potential gradient and/or electric potential is the driving force for separation.<sup>1,2</sup> Chemical potential is a function of pressure, concentration, and temperature.<sup>3</sup> As the vast majority of MSPs are athermal processes, the chemical potential can be expressed in terms of pressure gradient and concentration.<sup>1–3</sup> Electric potential is used as a driving force in electrodialysis.<sup>4</sup> Processes that employ pressure as the driving force are microfiltration (MF), ultrafiltration (UF), nanofiltration (NF), and reverse osmosis (RO).<sup>1–3,5</sup> During an NF process, usually pressure is applied in the range of 0.5–2.5 MPa.<sup>1–5</sup> An increase in pressure increases permeate flux and salt rejection; at the same time, it also increases concentration of the solute at the membrane surface, leading to polarization concentration and a decrease in the flux.<sup>3</sup> Application of an operating pressure is recommended where the flux is not affected by the increase of pressure.<sup>3</sup> Therefore, choice of experimental conditions is crucial for evaluating the performance of an MSP.

The separation process takes place through a combination of two mechanisms: ion size exclusion and ion charge exclusion.<sup>1–3</sup> Most NF membranes present a negative electrical charge in an aqueous medium, i.e., these membranes are negatively charged at neutral to alkaline pH and positively charged at low pH.<sup>4</sup> Separation takes place mainly via size exclusion and electrostatic interactions between the membrane and charged species. When the membrane surface is negatively charged, anions such as  $\text{SO}_4^{2-}$  and  $\text{PO}_4^{3-}$  tend to be rejected due to an increase in electrostatic repulsive forces; rejection of monovalent ions (such as  $\text{Cl}^-$ ) occurs basically via size exclusion effect. Thus, charge is an important parameter for retention in NF.<sup>3,4</sup> The Donnan effect is an interface phenomenon observed in charged membranes, thus contributing to the separation process, and is described in the equilibrium theory of semipermeable membranes.<sup>3</sup>

Usually, NF membranes are obtained in two stages: preparation of a microporous support and deposition of a thin film; usually a thin film of thickness between 0.1 and 0.5  $\mu\text{m}$ , which is responsible for

the rejection of membrane, is created by interfacial polymerization. Knowledge of the physicochemical properties of this film is crucial to determine the behavior of an NF membrane,<sup>6</sup> including its long-term performance.<sup>7</sup> In general, several techniques are used together to characterize virgin and used NF membranes. Among these,<sup>6</sup> membrane zeta potential is useful for correlating the transport of organic and inorganic solutes through NF membranes, as well as the flux performance and fouling behavior of a membrane.<sup>8</sup>

NF processes are used widely in seawater desalination, purification of enzymes, and concentration of fruit juices, among others, because they are able to reject negative multivalent ions, whereas monovalent ions are less rejected.<sup>3</sup>

Application of the membrane technology to treat low- and intermediate-level liquid radioactive wastes (LRWs) is relatively new.<sup>5,9–14</sup> Some articles have reported that RO and NF membranes showed 80–99.5% uranium rejection.

Initially, a set of experiments should be performed to evaluate the membrane processes to be used for treating radioactive waste before their implementation in a nuclear installation. For a membrane process to be competitive with conventional technologies, the former needs to operate with a high rate of flux, and present a high degree of selectivity and high resistance to fouling.<sup>15</sup> The NF membrane should be chosen such that it is chemically resistant and stable to radiation, as it will be exposed continuously to radioactive waste. Polyamide NF membranes meet these requirements because of their numerous intermolecular crosslinkings.<sup>16,17</sup> The pore size of an NF membrane is in the range of 1–10 nm, and the membrane is very stable between pH 2 and 11. In the nuclear area, depending on the composition, nature of the ion, and activity of the waste to be treated, performance of the membrane may change, resulting in a loss of its properties.

Some papers focused on the treatment of LRWs containing radionuclides, such as  $^{137}\text{Cs}$ ,  $^{241}\text{Am}$ ,  $^{238}\text{U}$ , and  $^{235}\text{U}$ , using NF membranes,<sup>14,18</sup> which reported over 80% rejection. However, membrane characterization before and after waste treatment has scarcely been studied. Long-term tests are also essential to decide the viability of NF as a separation technique to recover radionuclides from radioactive waste. Such studies are useful to determine possible changes in the membrane structure. Therefore, it is necessary to study various

\*e-mail: julio@iq.ufrj.br

parameters related to the operation before using a membrane separation process to treat a given radioactive waste.

For these reasons, this work aimed at evaluating the potential of an NF membrane in treating an LRW to recover the radionuclides present in it ( $^{235}\text{U}$  +  $^{238}\text{U}$ ). Transport properties (permeate flux, hydraulic permeability, and rejection) of an NF membrane were evaluated in two types of experiments: (a) short- and long-term static tests and (b) dynamic tests. After conducting the experiments for transport properties, chemical composition and morphology of the selective layer of the NF membranes were also evaluated.

## EXPERIMENTAL

### Radioactive waste sample

The sample of LRW was kindly provided by the Nuclear Fuel Factory at INB, which is responsible for the production of nuclear fuel for a pressurized water reactor (PWR), adopted in Brazil for electricity generation. This waste is generated after conversion of uranium hexafluoride ( $\text{UF}_6$ ) gas into uranium dioxide ( $\text{UO}_2$ ). The reaction of  $\text{UF}_6$  with carbon dioxide ( $\text{CO}_2$ ) and ammonia ( $\text{NH}_3$ ) produces ammonium tricarbonyluranate(VI), known as TCAU.<sup>18–20</sup> TCAU is dried in filters, generating a liquid waste containing uranium, known as “carbonated water” because of its high concentration of  $\text{CO}_3^{2-}$  ions. This waste was used as such for the experiments. Uranium was determined by the arsenazo(III) method<sup>21</sup> using a FEMTO 800 XI spectrophotometer ( $\lambda = 650 \text{ nm}$ ). The concentration of carbonate was determined by acid–base titration,<sup>22</sup>  $\text{NH}_3$  by the Nessler method,<sup>23</sup> and fluoride ions using an ion-selective electrode. The pH was determined using a Digmed DM-22 digital pHmeter.

### Membrane samples

The NF membrane used in this study was a commercial prototype developed for water desalination. It presents a selective layer of polyamide on a poly(ether sulfone) support and was identified as SW0 in this work. The membranes used in this work were kindly provided by Dow/Brazil. The molecular weight cutoff (MWCO) ( $600 \text{ g mol}^{-1}$ ) was determined using polyethyleneglycol (PEG).<sup>1,3,5</sup>

### Transport properties of the membranes

#### Permeate flux and hydraulic permeability

For the experiments involving permeate flux, hydraulic permeability, and rejection, a Pyrex solvent-resistant stirred XFOFU7601 cell filtration system (Millipore), with a flat membrane (active area =  $40 \text{ cm}^2$ ), was used. This system comprises a 350 mL cell, a magnetic stirring unit, and a feed tank (800 mL). The maximum operating pressure is 0.6 MPa; therefore, experiments were conducted under a pressure limit of 0.5 MPa. The system was pressurized using dry compressed air to carry the solution from the feed tank to the cell. Permeation experiments were conducted at a constant transmembrane pressure (0.1–0.5 MPa) and a stirring rate of 200 rpm. The permeation cell used in this work has been described in detail elsewhere.<sup>24</sup>

Circular membrane samples (diameter = 76 mm) were used for this study. Initially, the membrane was placed in water for an hour before being placed in the cell. The cell was filled with distilled water at 0.5 MPa to compact the membrane, which is necessary for accommodating the structure at the operating pressure. Compaction is achieved when three readings of the permeate flux at 20 min intervals become identical. The same procedure was carried out at pressures of 0.4, 0.3, 0.2, and 0.1 MPa. Value of the permeate flux ( $J_p$ ) of the

membrane was calculated using Eq. (1):<sup>2</sup>

$$J_p (\text{L m}^{-2} \text{ h}^{-1}) = \frac{\text{Flow} (\text{L s}^{-1}) \times 3600 (\text{s/h})}{\text{membrane area} (\text{m}^2)} \quad (1)$$

Data obtained were used to plot permeate flux versus pressure; slope of the line obtained is the hydraulic permeability of the membrane.

#### Rejection of chloride and sulfate ions

Behavior of the membrane toward chloride and sulfate ions was determined using sodium chloride ( $1000 \text{ mg L}^{-1}$ ) and sodium sulfate ( $1000 \text{ mg L}^{-1}$ ) solutions at pH 7 and 0.5 MPa. After determining hydraulic permeability, water was replaced with sodium chloride solution. The first 50 mL was discarded. A new aliquot of 50 mL was taken out and reserved together with a sample of the feed chloride solution. For estimating the rejection of sulfate ions, the cell was washed with deionized water at 0.5 MPa and filled with sodium sulfate solution, and the same procedure described above was repeated. Concentrations of chloride and sulfate ions in the feed and permeates were determined from their conductivity (using a Digmed DM-23 digital conductivity meter). Performance of the membrane was evaluated using the rejection factor ( $R$ , which is defined as the fraction of solute retained by the membrane for a given concentration of feed solution), as given in Eq. (2):<sup>2</sup>

$$R(\%) = \frac{C_f - C_p}{C_f} \times 100 \quad (2)$$

where  $C_f$  and  $C_p$  represent solute concentrations in the feed and the permeate, respectively. Conductivity readings of chloride and sulfate ions were fit to the respective analytical curves for calculating  $R$  values.

### Chemical stability of the membrane to the radioactive waste

Two different tests were performed: static and dynamic. The membrane was evaluated via short- (24–72 h) and long-term (288 and 5000 h) tests. Samples were immersed in 250 mL of the LRW in a closed system at 25 °C. Later, the test the sample was removed from the waste and washed with deionized water to determine permeate flux and rejection of chloride and sulfate ions. A thin film was created by the membrane that remained in the waste for 5000 h. The film was separated, washed with deionized water, centrifuged, washed with acetone, and dried at 25 °C for analysis.

The dynamic test was carried out using the same cell filtration system.<sup>24</sup> First, the permeate flux of a circular sample of the SW0 membrane was determined as described earlier. The cell was then filled with 250 mL of waste under magnetic stirring at 0.5 MPa. A volume of 50 mL of the permeated waste was taken after 24, 48, and 72 h. Concentration of uranium in the permeate was determined spectrophotometrically.<sup>21</sup>

### Morphological and chemical structure of the surface layer

#### Field emission scanning electron microscopy (FE-SEM)

The membrane was immersed in ethanol for 24 h, followed by immersion in *n*-hexane for another 24 h, and dried at 25 °C for 30 min, followed by drying at 60 °C for another 30 min. This procedure is carried out to avoid the collapse of the porous surface due to the high surface tension of water. The treated sample was placed on a sample holder and coated with gold to provide electrical conductivity to the membrane. The top surface morphology of the membrane was studied using a JEOL JSM6710F microscope.

### Attenuated total reflection Fourier transform infrared spectroscopy (ATR-FTIR)

ATR-FTIR spectra were obtained using a Nicolet 6700-Thermo Scientific instrument equipped with a ZnSe crystal at an incidence angle of 45° (0.4-0.6 µm depth).<sup>6,25</sup> Each spectrum results from 64 scans collected in the range of 650-4000 cm<sup>-1</sup> with a resolution of 2 cm<sup>-1</sup> at 25 °C.

The layer was isolated from the membrane after the 5000 h static test and analyzed by FTIR (KBr pellets) using a Thermo Scientific Nicolet 6700 spectrometer. Each spectrum was obtained as the average of 16 scans in the range of 4000-500 cm<sup>-1</sup> with a resolution of 4 cm<sup>-1</sup> at 25 °C.

### Atomic force microscopy (AFM)

AFM images were taken using a WITec Raman Sensitivity instrument. A silicon cantilever with a nominal tip apex radius of 10 nm was used to scan the membrane surface morphology at the contact mode. This technique allows the estimation of membrane roughness.<sup>26,27</sup> Images were obtained over an area of 2 × 2 µm<sup>2</sup> for three different surfaces, for both before and after immersion of the membrane in the waste. The images were analyzed using WITec Project 2.02 AFM image software.

### X-ray fluorescence (XRF)

Membranes were analyzed by an X-ray fluorescence spectrometer (EDXRF-800HS Shimadzu) equipped with a Si(Li) detector and a rhodium X-ray tube.

### Thermogravimetric analysis (TGA)

TGA was carried out using a NETZSCH STA 409 analyzer under an argon flux (5 mL min<sup>-1</sup>), at a heating and cooling rate of 10 °C min<sup>-1</sup> between 10 and 900 °C. Aluminum oxide (Al<sub>2</sub>O<sub>3</sub>) was used as a reference. The selective layer of each membrane was removed from the support using the following procedure: the membrane was placed in N,N-dimethyl acetamide (DMA) for a few minutes until complete dissolution of the support [poly(ether sulfone)]; the selective layer was removed and washed with acetone and dried at 25 °C. Ten milligram of the sample was placed in an Al<sub>2</sub>O<sub>3</sub> crucible. TGA analysis allows evaluation of the behavior of the selective layer of polyamide before and after exposure to waste.<sup>28</sup>

## RESULTS AND DISCUSSION

### Composition of the waste

Composition of an LRW is given in Table 1. It is evident from the table that uranium concentration (8 mg L<sup>-1</sup>) is fairly high and much above the limit for disposal in the environment (2 × 10<sup>-2</sup> mg L<sup>-1</sup>), as established by the Brazilian Environmental Agency.<sup>29</sup> However, this waste can be regarded as a useful source for recovery of uranium because of its significant average production in a batch process (1.3 × 10<sup>3</sup> L day<sup>-1</sup>) at INB.

**Table 1.** Concentration of uranium and chemical species (mg L<sup>-1</sup>) in the waste (pH 9.4)

U (uranium)	F <sup>-</sup> (fluoride ion)	CO <sub>3</sub> <sup>2-</sup> (carbonate ion)	NH <sub>4</sub> <sup>+</sup> (ammonium ion)
8.0 × 10 <sup>0</sup>	5.2 × 10 <sup>2</sup>	9.8 × 10 <sup>4</sup>	7.0 × 10 <sup>4</sup>

### Transport properties and rejection of the SW membrane

Figure 1 shows the graph of permeate flux versus pressure for

three circular SW0 membrane samples (SW1, SW2, and SW3). The slope gives the hydraulic permeability of each sample; the mean value was found to be 68 ± 8 L m<sup>-2</sup> h<sup>-1</sup> MPa, which falls in the upper limit of permeability values for NF membranes found in the literature (10–66 L m<sup>-2</sup> h<sup>-1</sup> MPa).<sup>1–3</sup> The hydraulic permeability of the membrane can be correlated with the monomer used in the selective layer. NF membranes usually have a selective layer of polyamide, which is hydrophilic.<sup>2,3</sup>

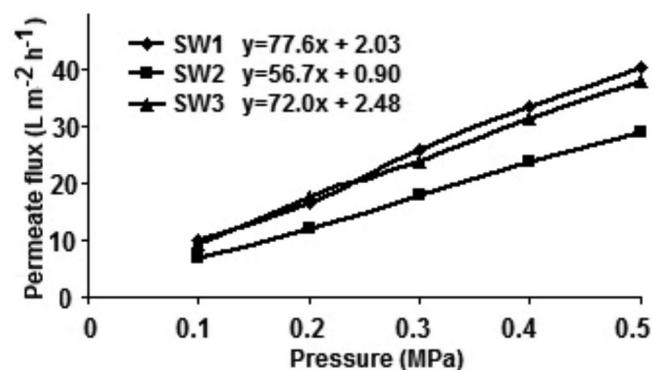


**Figure 1.** Graph of the permeate flux versus pressure of SW0 circular samples

The permeate flux and rejection of chloride and sulfate ions are shown in Table 2. Behaviors of the five SW0 samples with respect to permeate flux and rejection of sulfate ions are comparable, but rejection of chloride ions varied considerably (2.3–15%). In general, thin films of NF membranes are synthesized through interfacial polymerization, which occurs at the interface between two immiscible solvents.<sup>3</sup> During this process, performance of the membrane is affected by its surface irregularities.<sup>3</sup> Concentration polarization did not influence permeate flux of the membranes during these tests because this parameter was determined using water alone. Rejection of NF membranes is associated with the pore size distribution (Cl<sup>-</sup>)<sup>30</sup> and amount of charge on the membrane surface (SO<sub>4</sub><sup>2-</sup>).<sup>31</sup> Most of these membranes present a negative surface charge in aqueous media above pH 3.<sup>7,30–34</sup>

**Table 2.** Rejection factors and permeates flux of SW membranes before and after conditioning in the waste for several periods (P = 0.5 MPa)

Membrane	Permeate flux (L m <sup>-2</sup> h <sup>-1</sup> )	Rejection (%)	
		Cl <sup>-</sup>	SO <sub>4</sub> <sup>2-</sup>
SW-0	33.4 ± 6.2	9.0 ± 5.5	98.5 ± 0.5
SW24h	39.8 ± 4.8	3.6 ± 2.7	98.2 ± 0.1
SW-0	28.4 ± 1.0	15.1 ± 0.9	99.2 ± 0.6
SW48h	34.0 ± 1.4	8.5 ± 0.9	99.0 ± 0.4
SW-0	26.6 ± 4.2	12.9 ± 1.8	99.1 ± 0.2
SW72h	29.9 ± 4.8	10.0 ± 2.0	99.0 ± 0.2
SW-0	29.3 ± 0.6	9.3 ± 0.8	96.0 ± 0.5
SW288h	31.2 ± 0.5	7.0 ± 1.9	94.0 ± 0.4
SW-0	28.0 ± 0.1	2.3 ± 0.4	97.8 ± 0.4
SW5000h	28.7 ± 1.1	2.3 ± 1.1	63.3 ± 0.4

### Static tests

The data in Table 2 indicate that the permeate flux of the membranes increased after immersion in the waste, although this phenomenon was less pronounced after 288 and 5000 h.

Although rejection of sulfate ions by the membrane did not change significantly after short-term tests (24–72 h), it tended to decrease after long-term tests (288–5000 h). These results suggest that charge density of the membrane was altered by the waste after long periods of exposure. On the other hand, rejection of chloride ions decreased except after a very long time (5000 h). The difference in rejection of chloride ions before (SW0) and after immersion in the waste decreased with time (24–288 h): 60% after 24 h, 45% after 48 h, and 25% after 72–288 h. However, the trend was different for complete loss of a layer from the membranes after 5000 h, since this phenomenon took place only after immersion of the membrane for a very long time in the static tests.

The different results found in static tests suggest that membrane porosity was altered. In case of chloride ions (monovalent anions), size exclusion prevailed,<sup>30,31</sup> whereas for sulfate ions (divalent anions), rejection occurred mainly through charge exclusion mechanism.<sup>3</sup> Further tests are in progress to better understand the differences between rejection of sulfate and chloride ions.

Figure 2 shows typical AFM images (in gray scale) of the membrane surface; the light areas indicate smooth regions on the surface and dark areas represent pores/depressions.<sup>35</sup> Roughness of the membrane, which is one of the most important surface properties due to its strong influence on membrane behavior such as fouling, can be assessed using three-dimensional (3D) images.<sup>33</sup>

Topography of the SW24–72h membrane shows different morphologies when compared to the SW0 samples. Three-dimensional images (4  $\mu\text{m}^2$ ) of the SW0, SW24h, SW48h, and SW72h membranes (Figures 2a–2d) show a surface containing many thin peaks, which are account for the membrane roughness. The root mean square roughness values (Rms) of the membranes were 2.206, 28.670, 1.843, and 13.442 nm, respectively. The minimum peak was found for the SW48h (−6.422 nm) and the maximum for the SW24h (197.605 nm) sample. AFM images and roughness values indicate that immersion in the waste changed the surface layer of the membrane, showing an increase in roughness as compared to the SW0 membrane (Figure 2a).

### Rejection of uranium in dynamic tests

The “carbonated water” waste contains high amounts of carbonate ions (Table 1), which act as a strong complexing agent for uranium, forming different complex ions, depending on pH.<sup>12</sup> At pH 9.4, the dominant species is  $[\text{UO}_2(\text{CO}_3)_3]^{4-}$ . From literature data,<sup>6,8</sup> the NF membrane has a negative charge in the selective layer at this pH, indicating significant rejection of uranium by the membrane.

Table 3 presents uranium rejection at the membrane and the initial and final permeate fluxes. As expected, the SW membrane rejected 94% of uranium during short-term dynamic tests. After 5000 h, rejection was lowered to 73%. The decrease of uranium rejection seems to correlate with the lower sulfate rejection (Table 2), since both are multivalent anions.

The permeate flux was almost constant after 24–72 h but increased significantly after 5000 h, which can be explained by the loss of the coating layer of the membrane after this long test period.

### Characterization of the membrane surface

#### ATR-FTIR data

Spectra of the membranes before and after conditioning for 24, 48, and 72 h in the radioactive waste are presented in Figure 3a. Since the spectra are overlapped, the profiles are comparable among themselves and with those of the original membrane (SW0). This suggests that the integrity of the membranes was not much affected after exposure to the radioactive waste for short times. The characteristic N–H

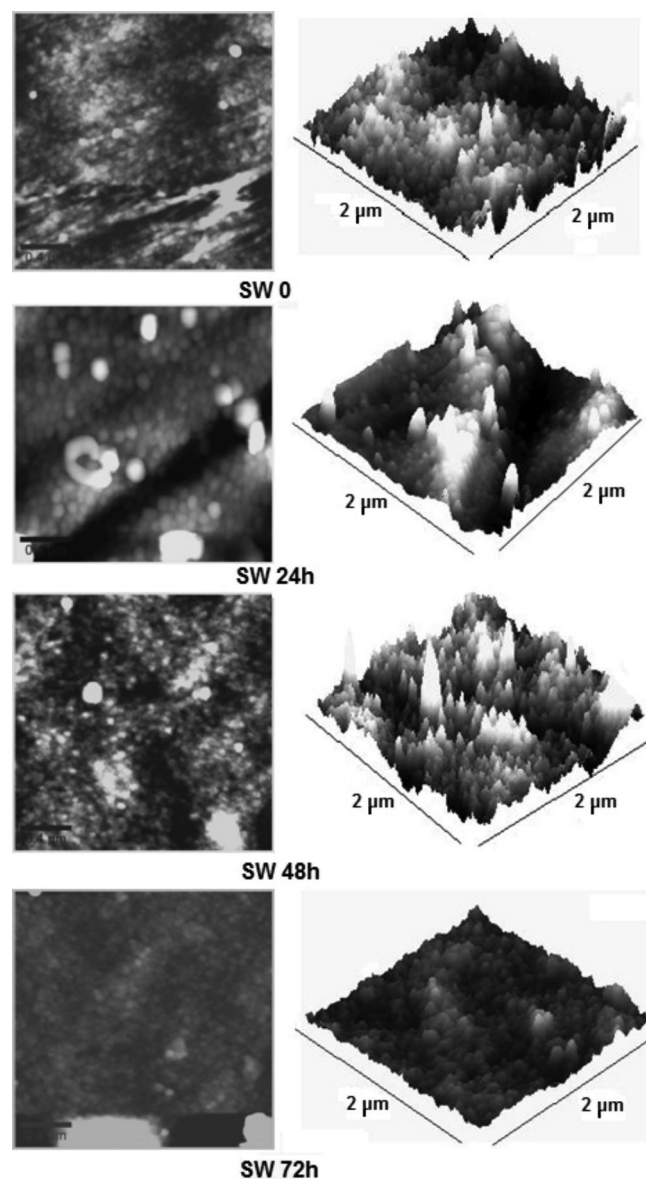


Figure 2. AFM images of SW0, SW24h, SW48h and SW72h membranes

Table 3. Uranium rejection and permeate flux of the SW membrane after dynamic tests

Uranium rejection (%)	Time (h)	Permeate flux* (L m <sup>-2</sup> h <sup>-1</sup> )
94.0	24	2.4
88.1	48	2.2
82.3	72	2.3
73.0	5000	43.0

\* Initial permeate flux: 2.6 L m<sup>-2</sup> h<sup>-1</sup> (after 3 h).

polyamide (3500–3200 cm<sup>-1</sup>), C–H aliphatic (~2900 cm<sup>-1</sup>), C=O, and aromatic ring (1700–1550 cm<sup>-1</sup>) bands are well noticeable.

Spectrum of the membrane after being immersed in the waste for 5000 h (Figure 3b) is different from the spectra of previous cases (Figure 3a). In particular, the band in the region 3500–3200 cm<sup>-1</sup> almost disappeared. As cited earlier, an external layer separated itself from the membrane. Its IR spectrum (Figure 4) shows strong bands at ~3400 cm<sup>-1</sup>, which are characteristic of O–H stretching from inter- and intramolecular hydrogen bonds; the bands at 2900,

1655, 1144, 1095, and 919  $\text{cm}^{-1}$  correspond to the major polyvinyl alcohol (PVA) absorption bands,<sup>36</sup> with the one at 1144  $\text{cm}^{-1}$  being assigned to the degree of crystallinity of PVA.<sup>37</sup> Therefore, the layer recovered from the SW membrane is a PVA coating layer, the main objective of which is to form a smoother membrane surface.<sup>7</sup> This result agrees with literature data,<sup>7,38</sup> and also correlate very well with AFM (Figure 2) and ATR-FTIR (Figure 3) data.

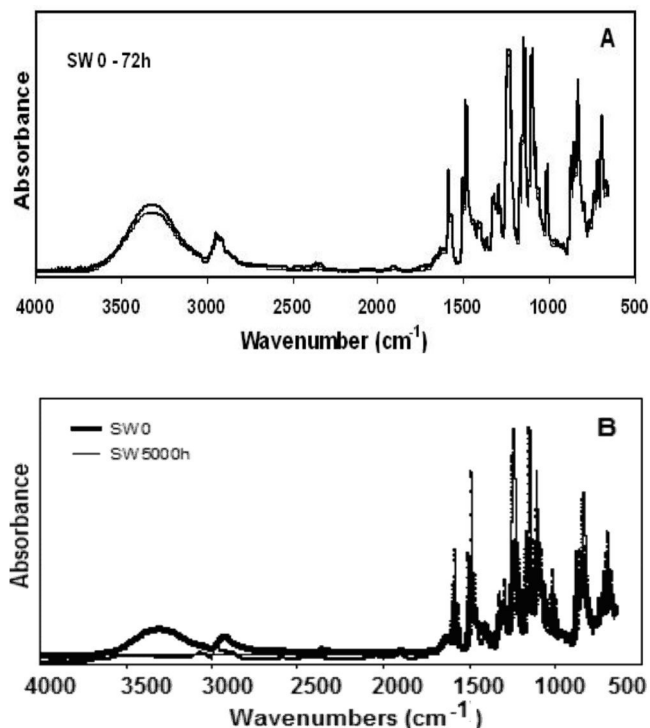


Figure 3. ATR-FTIR spectra of the SW membrane before and after conditioning in the waste for (a) 0, 24, 48 and 72 h and (b) 0 and 5000 h

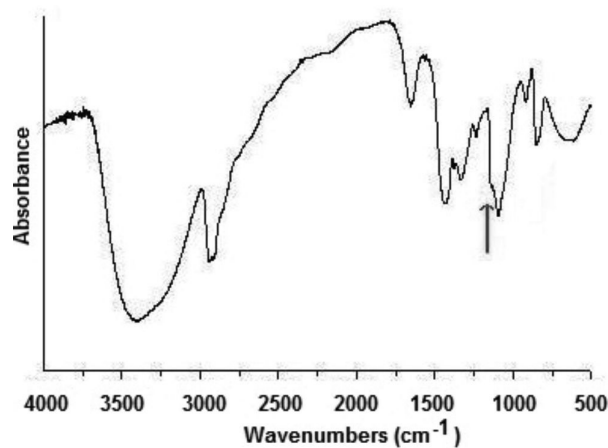


Figure 4. FTIR of the layer recovered from the membrane after conditioning in the waste for 5000 h

#### FE-SEM data

Morphological aspects of the SW0 and SW72h membrane surfaces before and after immersion in the waste are presented in Figures 5(a) and (b), respectively. The initial (SW0) membrane surface appears to be completely smooth without apparent porosity, even after a magnification of 100,000 $\times$ . After immersion in the waste for 72 h, the membrane surface presents some morphological changes, showing many agglomerates (with an average size of 100 nm). The external layer (PVA) appears to be segregated at some regions, thereby

exposing part of the selective layer directly to the waste. This phenomenon took place prior to the release of the PVA layer after 5000 h, as seen earlier (Figures 3 and 4).

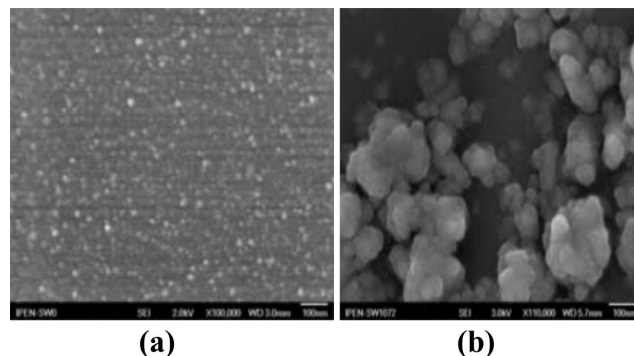


Figure 5. Micrographs of the SW0 (a) and SW72h (b) membrane surface (magnification: 100,000 $\times$ )

#### XRF data

An analysis of the SW72h membrane data (Figure 6) shows the presence of titanium. The use of this element in polymeric and ceramic membranes as an antibacterial agent is well known.<sup>39,40</sup> It is usually employed in the form of nanoparticles, which are incorporated into the covering layer of the membranes used for desalination.<sup>5</sup> Titanium increases membrane resistance to compaction, but does not alter its flux or ion rejection.<sup>40</sup>

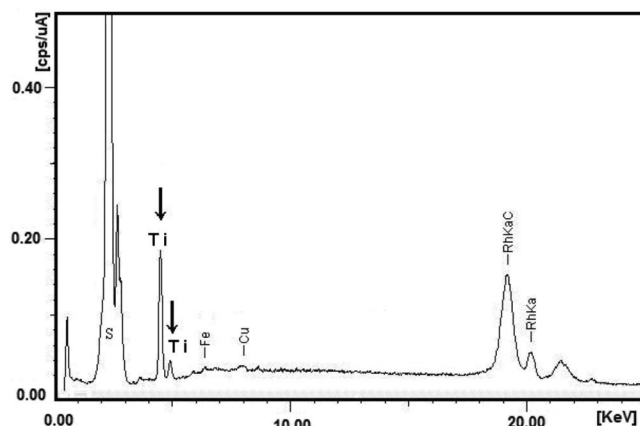


Figure 6. XRF of the SW72h membrane

#### TGA of the selective layer

TGA of the selective layer provides information regarding weight loss in the samples in two different forms: weight loss as a function of the temperature and derivative of weight loss as a function of temperature (DTG). Figures 7(a)–(d) present the TG curves of the polyamide layer not exposed (SW0) and exposed (SW24–72 h) to the waste. Degradation of the SW0 membrane occurred in two well-defined steps. The first stage was observed between 240 and 519.5  $^{\circ}\text{C}$  ( $\sim 20\%$  weight loss), mainly involving water removal and formation of volatile organic compounds followed by dehydration of hydroxyl groups. PVA degradation (220  $^{\circ}\text{C}$ ) occurs in this stage.<sup>41</sup> The second decomposition stage (519.5–900  $^{\circ}\text{C}$ ) corresponds to thermal (breaking of the chains, release of volatile products, and formation of residues) and oxidative degradation of carbonaceous residues, with a maximum rate of weight loss occurring at 663  $^{\circ}\text{C}$ . The similarity of the TG plots of the SW24–72h samples correlate very well with ATR-FTIR data (Figure 3). The first decomposition stage of the SW24h sample was completed around 230  $^{\circ}\text{C}$  ( $\sim 20\%$

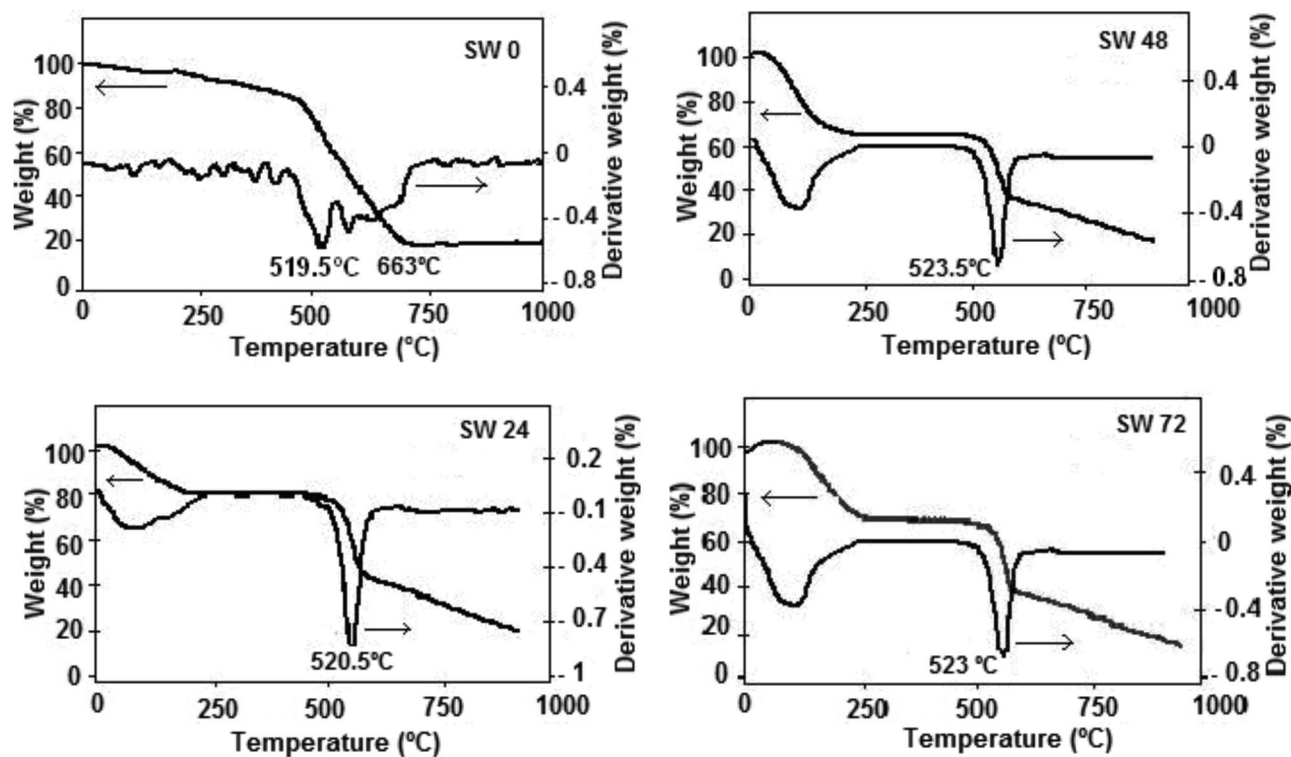


Figure 7. TG and DTG of the surface layer of polyamide of the SW membrane before and after immersion in the waste for 0, 24, 48 and 72 h

weight loss), followed by a plateau until 520.5 °C. Weight loss in the second stage (520.5–900 °C) was smoother than that for the SW0 sample. The first stage of the SW48–72h membranes was completed by around 250 °C (~30% weight loss), followed by a plateau until 523 °C. The second stage (523–900 °C) showed the same trends as observed for the SW24h sample.

TGA clearly suggests that the polyamide layer of the SW24–72h membranes exposed to the waste is less thermally stable than the SW0 membrane. This result is consistent with the literature data.<sup>16,17,42,43</sup>

## CONCLUSIONS

Contact of the membrane with the waste altered its transport properties. The permeate flux increased after exposure to the radioactive waste, but this increase was lowered as the immersion time increased. Rejection of chloride ions decreased, especially after immersion of the membrane in the waste for short times (24–48 h). Rejection of sulfate ion was reduced clearly only after a very period of exposure (5000 h), when the PVA coating layer was lost.

NF seems to be a promising technique for the recovery of uranium from an LRW. After dynamic tests for 5000 h, 73% of uranium present in a LRW was rejected despite the loss of the PVA coating layer and a huge increase of the permeate flux was observed. However, other commercial or laboratory-made NF membranes (with different selective layers and special configurations) should be tested to determine the sample that is most stable in contact with the waste under study. Tests using tangential fluxes should be performed, since they resemble those found in industrial plants, where the operating pressure may reach 7.0 MPa. These tests are essential for the transition of a process from the laboratory scale to the pilot plant or industrial scale.

## ACKNOWLEDGMENTS

We acknowledge INB for providing the waste, the Instituto de Química/UFRJ for FTIR analysis, and COPPE/UFRJ for AFM

analyses. The membranes used in this work were kindly provided by Dow/Brazil.

## REFERENCES

- Nath, K.; *Membrane separation processes*, Prentice-Hall: New Delhi, 2008.
- Mulder, M.; *Basic principles of membrane technology*, 2<sup>nd</sup> ed., Kluwer Academic Publishers: Dordrecht, 2000.
- Schäfer, A. I.; Fane, A. G.; Waite, T. D. *Em Nanofiltration: principles and applications*; Schäfer, A. I.; Fane, A. G.; Waite, T. D., eds.; Elsevier: Oxford, 2005.
- Tanninen, J.; Platt, S.; Weiss, A.; Nyström, M.; *J. Membr. Sci.* **2004**, *240*, 11.
- Dulama, M.; Deneanu, N.; Dumitru, E.; Popescu, I. V.; Pavelescu, M.; *Proceedings of NUCLEAR 2008 annual international conference on sustainable development through nuclear research and education*, Pitesti, România, 2008, p. 426-433.
- Tang, C. Y.; Kwon, Y. N.; Leckie, J. O.; *J. Membr. Sci.* **2007**, *287*, 146.
- Tang, C. Y.; Kwon, Y. N.; Leckie, J. O.; *Desalination* **2009**, *242*, 149.
- Childress, A. E.; Elimelech, M.; *Environ. Sci. Technol.* **2000**, *34*, 3710.
- Macnaughton, S. J.; McCulloch, J. K.; Marshall, K.; Ring, R. J.; *Technologies for the treatment of effluents from uranium mines, mills and tailings*, Viena, Áustria, 2002, p. 55-65.
- Gra yna, Z. T.; *J. Membr. Sci.* **2003**, *225*, 25.
- Pabby, A. K.; *Membr. Technol.* **2008**, *2008*, 9.
- Raff, O.; Wilken, R. D.; *Desalination* **1999**, *122*, 147.
- Lin, K. L.; Chu, M. L.; Shieg, M. C.; *Desalination* **1987**, *61*, 125.
- Ambashta, R. D.; Sillanpää, M. E. T.; *J. Environ. Radioact.* **2012**, *105*, 76.
- Chennamsetty, R.; Escobar, I.; Xu, X.; *J. Membr. Sci.* **2006**, *287*, 146.
- Chmielewski, A. G.; Harasimowicz, M.; *Nukleonika* **1992**, *37*, 61.
- Chmielewski, A. G.; Harasimowicz, M.; *Nukleonika* **1997**, *42*, 857.
- Oliveira, E. E. M.; Barbosa, C. C. R.; Afonso, J. C.; *Membrane Water Treatment* **2012**, *3*, 231.

19. Cunha, K. M. D.; Lima, C.; Leite, C. V. B.; Santos, M.; Carneiro, L.; Lima, R. M. G.; *J. Occup. Environ. Hyg.* **2011**, *8*, D51.
20. Mellah, A.; Chegouche, S.; Barkat, M.; *Hydrometallurgy* **2007**, *85*, 163.
21. Sawin, S. B.; *Talanta* **1961**, *8*, 673.
22. Harris, D. C.; *Quantitative chemical analysis*, 8<sup>th</sup> ed., W. H. Freeman and Company: New York, 2010, chap. 10.
23. ASTM Manual of water and environmental technology, D1426-93, "The Nessler Method", American Society for Testing Materials: New York, 1995.
24. Arthanareeswaran, G.; Starov, V. M.; *Desalination* **2011**, *267*, 57.
25. Nanda, D.; Tung, Kuo-Lun; Li, Yu-Ling; *J. Membr. Sci.* **2010**, *349*, 420.
26. Boussu, K.; Zhang, Y.; Cocquyt, J.; Van der Meeren, P.; Volodin, A.; Van Haesendonck, C.; Martens, J. A.; Van der Bruggen, B.; *J. Membr. Sci.* **2006**, *278*, 418.
27. Bowen, W. R.; Doneva, T. A.; *J. Membr. Sci.* **2000**, *126*, 91.
28. Singh, A. K.; Thakur, A. K.; Shahi, V. K.; *Desalination* **2013**, *309*, 275.
29. Brasil; Directory from the National Brazilian Environmental Council (CONAMA) n. 357, March 17, 2005, *Official Journal*, March 18, 2005.
30. Tanninen, J.; Manttari, M.; Nyström, M.; *J. Membr. Sci.* **2006**, *283*, 57.
31. Chang, E. E.; Huei, L. C.; Pao, H. C.; *Sep. Purif. Technol.* **2012**, *85*, 1.
32. Rautenbach, R.; Groschl, A.; *Desalination* **1990**, *77*, 73.
33. Skozi, S.; Patzay, G.; Weiser, L.; *Desalination* **2002**, *151*, 123.
34. Veríssimo, S.; Peinemann, K. V.; Bordado, J.; *J. Membr. Sci.* **2006**, *279*, 266.
35. Bowen, W. R.; Doneva, T. A.; *Desalination* **2000**, *129*, 163.
36. *Encyclopaedia of polymer science & technology*; Mark, H. F.; Gaylord, N.G.; Bikales, N. M., eds.; John Wiley & Sons: New York, 1969, vol. 14, p. 149-198.
37. Mansur, H. S.; Sadahira, C. M.; Souza, A. N.; Mansur, A. A. P.; *Mater. Sci. Eng., A* **2008**, *28*, 539.
38. Quanfu, A.; Li, F.; Ji, Y.; Chen, H.; *J. Membr. Sci.* **2011**, *367*, 158.
39. Benfer, S.; Popp, U.; Richter, H.; Siewert, C.; Tomandl, G.; *Sep. Purif. Technol.* **2001**, *22-23*, 231.
40. Lee, H. S.; Im, S. J.; Kim, H. J.; Kim, J. P.; Min, B. R.; *Desalination* **2008**, *219*, 48.
41. Sin, L. T.; Rahaman, W. A.; Rahman, A. R.; Mokhtar, M.; *Carbohydr. Polym.* **2011**, *83*, 303.
42. Ghosh, S.; Khastgir, D.; Bhowmick, A. K.; Mukunda, P. G.; *Polym. Degrad. Stab.* **2000**, *67*, 427.
43. Ramachandran, V.; Misra, B. M.; *J. Appl. Polym. Sci.* **1982**, *27*, 3427.